$^{36}S(d,p)^{37}S$ and $^{34,36}S(d,^3He)^{33,35}P$ reactions

C. E. Thorn, J. W. Olness, and E. K. Warburton
Brookhaven National Laboratory, Upton, New York 11973

S. Raman
Oak Ridge National Laboratory, Oak Ridge, Tennessee 37830
(Received 10 May 1984)

The $^{36}S(d,p)^{37}S$ reaction was studied at $E_d=25$ MeV with an enriched ^{36}S target (81.1%) and momentum analysis of the protons. Twenty-six groups were identified with levels in ^{37}S. Excitation energies were obtained with an uncertainty of $\lesssim 3$ keV and angular distributions yielded l and S values for the transfer reaction. Comparison is made to local systematics and the $l=1$ strength is also compared to recent (n,γ) results. The $^{34,36}S(d,^3He)^{33,35}P$ reactions were also studied. A mass excess for ^{35}P of $-24854(5)$ keV was obtained. $(d,^3He)$ proton pickup strength was observed to four states of ^{35}P and seven states of ^{33}P. These results are compared to predictions of Wildenthal.

I. INTRODUCTION

Recently, a quantity of ^{36}S enriched to $(81.1\pm0.2)\%$ (natural abundance $=0.017\%$) was produced in the Soviet Union and became available to physicists in the United States initially for studying the $^{36}S(n,\gamma)^{37}S$ reaction.[1] A $^{36}S(d,p)^{37}S$ experiment was planned simultaneously because of the need to resolve ambiguities in the ordering of the γ-ray cascades following thermal neutron capture. A preliminary version of the (d,p) study has been given.[2] Other studies of the $^{36}S(d,p)^{37}S$ reaction using targets fabricated from similar material have also been reported.[3–5]

Since ^{36}S has $Z=16,N=20$, the $^{36}S(d,p)$ reaction probes the structure of the $f_{7/2}$, $p_{3/2}$, $p_{1/2}$, and $f_{5/2}$ neutron orbits outside the closed $(2s,1d)$ neutron core. ^{37}S has valence neutrons and protons in different major shells, and shell-model calculations for this "crossed-shell" nucleus have not been made. However, the planning of such a calculation should be aided by the systematics of the relative binding energies of the (f,p) neutron orbitals as the proton shell is filled in the sequence ^{37}S-^{39}Ar-^{41}Ca. The extraction of (d,p) spectroscopic factors is necessary for the location of the (f,p) neutron strength and was therefore undertaken. As will be seen (Sec. III C), these spectroscopic factors also provide data for an interesting comparison between the (n,γ) and (d,p) reactions.

The $^{36}S(d,^3He)$ reaction allows the investigation of ^{35}P for which only the ground state is known.[6,7] Since the ^{36}S material contains $(18.8\pm0.1)\%$ ^{34}S, information on the $^{34}S(d,^3He)^{33}P$ reaction is obtained simultaneously with that for $^{36}S(d,^3He)^{35}P$. Predictions for the level structure and the $(d,^3He)$ spectroscopic factors exist[8] for both ^{33}P and ^{35}P.

II. EXPERIMENTAL PROCEDURES

A. Target

Previous experience[9] had shown that stable uniform targets of Ag_2S could be fabricated with relative ease. These were made by sulphiding Ag foils of 175 or 200 $\mu g/cm^2$. For 100% sulphiding, the ^{36}S thicknesses would be 23.7 and 27.0 $\mu g/cm^2$, respectively, for an enrichment of 81.1%. Past experience[9] and inspection of the targets by a microscope indicates nearly complete sulphiding and we assume $85\pm15\%$ of the Ag is converted to Ag_2S, yielding ^{36}S thicknesses of 20.1 ± 3.0 and 23.0 ± 3.4 $\mu g/cm^2$, respectively. The sulphur has a ^{34}S content of $(18.8\pm0.1)\%$ and thus the ^{34}S target thicknesses are 4.4 ± 0.7 and 5.0 ± 0.8 $\mu g/cm^2$, respectively. A ^{34}S enriched Ag_2S target was made at the same time to provide information on the background to the ^{36}S reactions.

B. Experimental procedure

The deuteron beam was provided by the BNL Double MP tandem facility and the proton and ^3He spectra were momentum analyzed in the BNL QDDD magnetic spectrometer. The solid angle of the spectrometer was 4.2 msr, subtending 3° in the reaction plane. Targets were mounted in a scattering chamber and the integrated beam intensity was monitored with a Faraday cup. The detector consisted of a multiwire proportional counter backed by a stopping plastic scintillator.[10] The (d,p) measurements were performed at $E_d=25$ MeV and the $(d,^3He)$ measurements at $E_d=30$ MeV.

These experiments were the first use of a deuteron beam at BNL since SF_6 was introduced into the tandems in 1975. It was found that at $E_d=25$ MeV activation of 14.26 d ^{32}P via the $^{32}S(n,p)$ reaction on the SF_6 was serious enough to demand a several week waiting period before any maintenance could be done inside the tandem tank. Thus, the latter part of the study was performed with N_2 in the pressure tank.

C. The $^{36}S(d,p)^{37}S$ spectra

The 15° spectrum from $^{36}S(d,p)^{37}S$ is shown in Fig. 1. Twenty-six proton groups corresponding to states in ^{37}S are labeled up to an excitation energy of 6.5 MeV. The

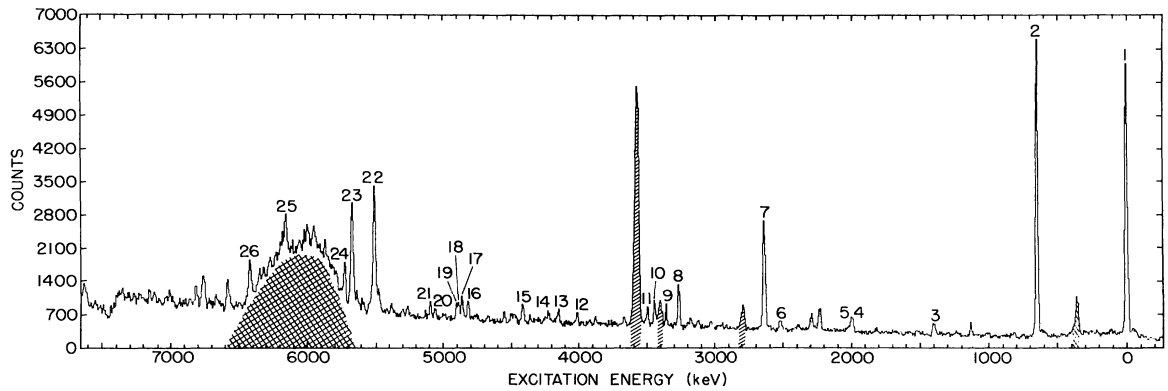

FIG. 1. Proton spectrum from ^{36}S(d,p)^{37}S. The proton groups corresponding to ^{37}S energy levels are numbered sequentially as in Tables I and IV. Contaminant groups are cross hatched. The very broad group arises from hydrogen in the Ag_2S target.

energy resolution of $\sim$15 keV full width at half maximum (FWHM) was due almost entirely to energy loss and straggling in the target. These 26 proton groups were observed at nine angles between 7° and 50° and were assigned to ^{37}S on the basis of their kinematic shift with angle. In addition, the spectra from the ^{34}S target were recorded simultaneously with those from ^{36}S for $\theta=15°$ and none of these 26 proton groups were seen in that spectrum. The excitation energies deduced for the 26 ^{37}S levels are listed in Table I where they are compared to previous values.[1,3,4,11] The assignment of these groups to ^{37}S is quite definite. An attempt was made to locate all ^{37}S proton groups which corresponded to bound levels, i.e., $E_x<4303$ keV, and which had non-negligible (>50 μb/sr) cross sections. As the excitation energy increases above 4.3 MeV, the probability of missing ^{37}S levels increases.

It was found that the background from Ag(d,p) was small and structureless. This was expected for three reasons. First, the Q values for ^{107,109}Ag(d,p) are 5.05 and 4.60 MeV, respectively, compared to 2.079 MeV for ^{36}S(d,p)^{37}S. Thus the region of excitation in ^{108,110}Ag covered is $\sim$2.5—9.0 MeV, where the level density is very high. Second, (d,p) cross sections for $A\sim110$ are small, relative to those for $A\sim36$, and finally, the QDDD kinematic compensation was tuned for an $A\sim36$ target so that the (d,p) reaction on $A\sim110$ targets had considerably worse resolution (also true for $A\sim12$ contaminants as illustrated in Fig. 1).

Data were collected at nine angles with six or seven momentum bites per angle. In order to obtain accurate reaction Q values it is necessary to determine the relationship between the position measured by the focal plane detector and magnetic rigidity. A procedure has been developed[12] to accomplish this calibration for the QDDD spectrometer. Measured corrections for magnet saturation and multipole field settings are applied to the measured fields and peak positions. If the magnets are properly cycled to remove the effects of hysteresis, the nonlinear terms in the calibration are independent of magnetic fields so that a global fit to all the data can be used. Hysteresis effects were eliminated by cycling the magnets at the beginning of the experiments, and only increasing the magnetic field slowly for successive measurements. Whenever a decrease in field was required, the magnets were again cycled.

The calibration resulting in the excitation energies of Table I was made from proton groups corresponding to ^{12}C(d,p)^{13}C, ^{16}O(d,p)^{17}O, ^{34}S(d,p)^{35}S, and ^{36}S(d,p)^{37}S. Q values and excitation energies for the first three listed reactions are accurately known. The ^{36}S(d,p)^{37}S Q value of 2078.95(12) keV is otained from the (n,γ) result[1] for the neutron separation energy, $S_n(^{37}S)=4303.52(12)$ keV. The ^{37}S excitation energies from the (n,γ) reaction (Table I) were also used. These various reactions have different enough kinematical shifts and Q values so that a least squares fit at a given angle determines the incident deuteron energy and the scattering angle as well as the energies of the proton groups. The excitation energies of Table I result from an average of the results from six angles plus a careful appraisal of the systematic errors. We believe the uncertainties assigned to these energies are realistic.

D. DWBA analysis

The experimental angular distributions were compared to the distorted wave Born approximation (DWBA) by means of the code DWUCK4.[13] The optical model parameters[14–16] used for both the (d,p) and (d,^{3}He) reactions are listed in Table II. In addition, the finite range correction factor was set to 0.695 and 0.770 for the (d,p) and (d,^{3}He) reactions, respectively. For the (d,p) reaction, a nonlocal correction was made with the parameter *PNLOC* of DWUCK4 set at 0.54 for the deuteron and 0.85 for the proton and transferred neutron. These values for the finite range and nonlocality parameters follow the recommendation of Kunz.[13] For the (d,^{3}He) reaction we follow the customary practice of not applying a nonlocality parameter. The effect of these two corrections is small for the shape of the angular distributions. Its effect on the absolute magnitude is illustrated in Table III. The experimental cross section was related to the cross section (σ_{DW}) calculated by DWUCK4 via

$$\sigma_{exp}(\theta)=N(C^2S)\sigma_{DW}(\theta)\ \text{mb/sr}\ , \qquad (1)$$

where,[13] for a spin zero target, $N=15.5$ for the (d,p) reac-

TABLE I. ^{37}S excitation energies.

No.[a]	^{37}S excitation energy (keV) and its uncertainty in the last digit				
	Present	Piskoř *et al.*[b]	(n,γ)[c]	Solin *et al.*[d]	(t,^{3}He)[e]
1	0	0	0	0	0
2	644.3(19)	645.85(17)	646.18(2)	642	647(15)
3	1395.0(19)	1397.93(33)	1397.51(18)	(1394)	1399(20)
	f			(1536)	
4	1993.3(31)	1991.11(24)	1991.93(5)	1991	
5	2023.8(29)	2020.90(45)	2022.87(10)	2024	2020(20)
6	2516.8(38)	2514.77(32)		(2514)	
7	2638.3(21)	2637.79(20)	2637.86(3)	2636	
	g	[2776.28(65)]			2775(15)
	g				2978(15)
	h	3169.85(30)			
	h	[3180.68(37)]			
8	3261.0(31)	3262.56(24)	3261.90(5)	3263	3262(15)
9	3356.0(17)	3355.41(35)		(3354)	3337(15)
10	3442.0(20)	3442.13(35)			3430(30)
11	3493.5(16)	3493.26(29)	3492.71(8)	3493	
12	4007.8(36)	4002.94(30)			
13	4150.5(37)	4147.0(18)			
14	4226.3(36)				
15	4407.7(26)				
16	4812.8(35)				
17	4853.8(23)				
18	4883.0(17)				
19	4903.0(54)				
20	5053.0(27)				
21	5086.3(39)				
22	5498.8(31)	5501.98(2)			
23	5662.3(35)	5663.90(67)			
24	5713.4(37)	5717.91(85)			
	h	5944.01(79)			
25	6150.2(23)	6149.2(17)			
26	6408.5(33)	6406.4(21)			

[a]The numbers correspond to those in Fig. 1. States above No. 14 are unbound.
[b]Reference 3. Levels in parentheses are uncertain. For all levels above 3400 keV a systematic error of $\sim$1.3 keV should be added to that given.
[c]Reference. 1.
[d]Reference 4. The quoted uncertainty for all energies in $\pm$6 keV. The authors considered the levels in parenthesis as uncertain.
[e]Reference 11.
[f]A 1536-keV level was not observed. A limit on its integrated 7°—50° cross section is $< \frac{1}{10}$ of that for the 1395-keV level.
[g]Not observed. The 7°—50° integrated cross section is less than 0.03 times that for the 2638 keV level.
[h]This peak would have been obscured by a ^{34}S(d,p) peak at forward angles, in any case it is relatively weak.

tion and $29.5/(2J_f+1)$ for the (d,^{3}He) reaction are recommended for use with the finite-range parameters listed above. In Eq. (1) C^2 is an isospin Clebsch-Gordan coefficient

$$C^2 = \langle T_A T_{ZA} t t_z \mid T_B T_{ZB} \rangle^2 , \quad (2)$$

where t, t_z refer to the transferred nucleon. For the ^{36}S(d,p)^{37}S, ^{36}S(d,^{3}He)^{35}P, and ^{34}S(d,^{3}He)^{33}P reactions

TABLE II. Optical model parameters. Well depths are in MeV and geometrical parameters in fm.

Particle	V	r_v	a_v	W	W'	r_w	a_w	$\vec{l}\cdot\vec{s}$	r_c	Ref.
Deuteron	91.3	1.170	0.752	0.80	34.82	1.325	0.721	13.2	1.3	14
Proton	46.2	1.142	0.728	1.84	25.08	1.308	0.645	19.7	1.2	15
^{3}He	177.2	1.140	0.710	15.6	0	1.660	0.829	0	1.4	16
Bound nucleon	a	1.200	0.650	0	0			$\sim$30[b]	1.2	

[a]Adjusted to give a binding energy equal to the experimental separation energy.
[b]The *VSOR* parameter of DWUCK4, λ, was set equal to 25.

C^2 is 1, $\frac{5}{6}$, and $\frac{3}{4}$, respectively. The spectroscopic factor S measures the overlap between $A+n$ and B.

E. ^{36}S(d,p)^{37}S angular distributions

Results for ^{36}S(d,p)^{37}S are shown in Figs. 2–4. $l=1$ transfer is assigned to four of the five levels on the right-hand side of Fig. 2. For the 3494-keV level $l=1$ is preferred but not definite. For the g.s. and 2517-keV levels shown on the left-hand side, an $l=3$ assignment is made, while $l=2$ is assigned to the 1395-keV level. The DWBA results for unbound levels were calculated with the neutron just bound. This assumption is not justified and so definite assignments cannot be made; however, it appears likely that the 5499-keV level (Fig. 2) is formed by $l=3$, while the data for the 4408-keV level can only be fit assuming $l=4$ (Fig. 3). Alternate l values for transfer to the 2024-keV level are shown in Fig. 4 to illustrate the degree of selection. The proton group corresponding to this level was only partly resolved from that for the more intense 1993-keV level. The comparison of Fig. 4 strongly favors an $l=3$ assignment.

The results are summarized in Table IV which lists the spectroscopic factors derived from a comparison of the data to DWUCK4. The S values were found to be quite insensitive to reasonable changes in the optical model parameters. For instance, small changes could be made in the parameters to obtain better fits for individual levels, but these changes had little effect on $\sigma_{DW}(\theta)$ near the maximum.

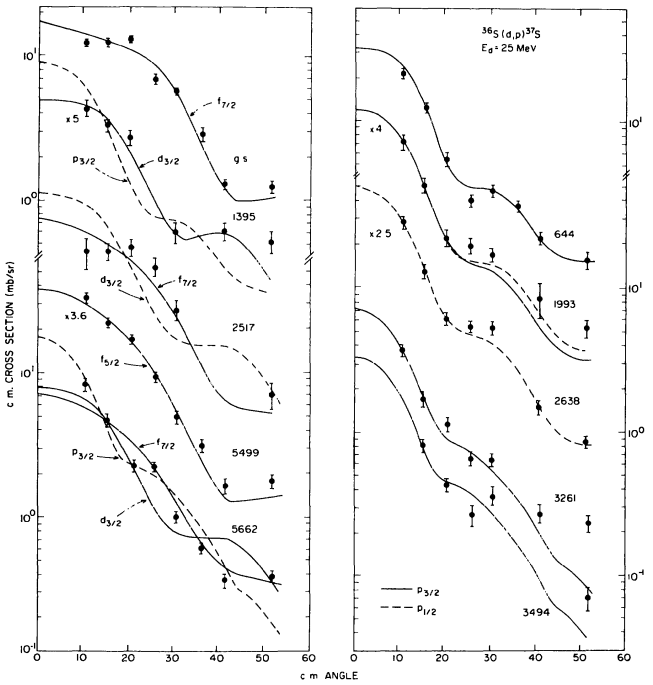

FIG. 2. Angular distributions for ^{36}S(d,p)^{37}S. The data are labeled by the excitation energy (in keV) of the final level. The theoretical curves are calculated with the distorted wave code DWUCK4 as discussed in the text. The curves on the right-hand side are all $l=1$ transfers, either $p_{1/2}$ or $p_{3/2}$ orbitals as indicated. Those on the left-hand side are labeled by the assumed orbit of the transferred neutron. The ordinate scale has an estimated uncertainty of 20%. The scale factors (e.g., $\times 5$) have been applied to the data. Comparison of the theoretical and experimental curves yields the spectroscopic factors of Table IV.

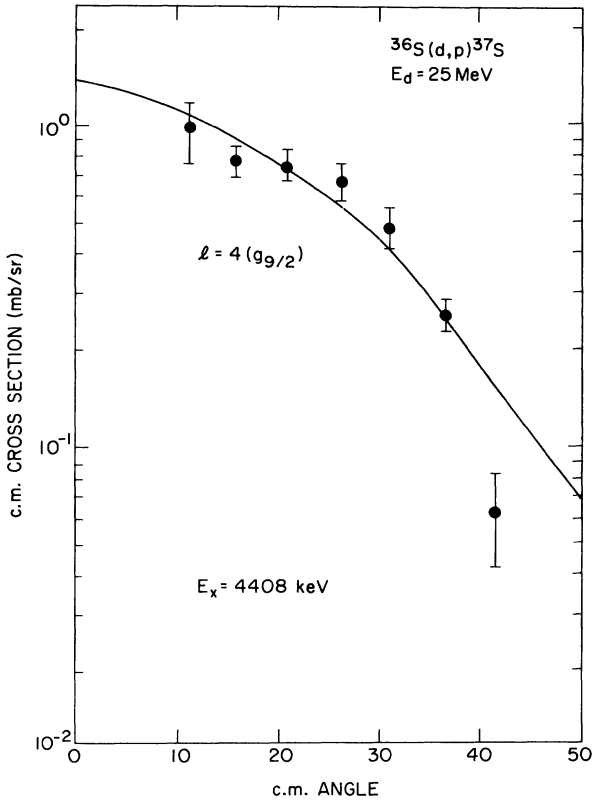

FIG. 3. Angular distribution for the ^{36}S(d,p)^{37}S 4408-keV level. The $l=4$ transfer is the only one for $l\leq 4$ which gives a reasonable fit. The cross section scale has an estimated uncertainty of 20%.

A check on the absolute cross section was provided by (d,p) data at $\theta_{lab}=10°$ where the proton groups corresponding to ^{34}S(d,p)^{35}S 1.99- and 2.35-MeV levels were observed. Comparison to a DWBA calculation using the parameters of Table II gave $(2J+1)S$ values for these two levels of 4.1 ($1f_{7/2}$) and 2.0 ($2p_{3/2}$), respectively, in satisfactory agreement with previous results.[6] Since the ^{34}S/^{36}S ratio is accurately known for the material used, this provides a check on the absolute cross section results for ^{36}S + d also.

The (d,p) and (d,^{3}He) cross sections have an estimated uncertainty of 20%. As is always the case it is difficult to ascribe an uncertainty to the extraction of spectroscopic factors via the DWBA. The minimum estimated uncertainty is ~25%, which may pertain for the (d,p) reaction proceeding to bound states. As is clear from Table III and Fig. 6, the $l=0$ (d,^{3}He) S values have a very large uncertainty (~ factor of 2), while the $l=2$ (d,^{3}He) S values are probably extracted with ~50% uncertainty.

TABLE III. Examples of the effect of the DWUCK4 finite range and nonlocality corrections.

Reaction	Final state (MeV)	J^π	$N\cdot\sigma_{DW}(\theta)$ in (mb/sr)[a] Finite range energy locality	Finite range nonlocality	No finite range energy locality	θ
^{36}S(d,p)^{37}S	0	$\frac{7}{2}^-$	16.2	19.3	16.3	16°
	0.64	$\frac{3}{2}^-$	34.5	39.8	33.7	10°
^{36}S(d,^{3}He)^{35}P	0	$\frac{1}{2}^+$	1.43	1.87	0.78	20°
	3.85	$\frac{5}{2}^+$	1.24	1.74	1.50	16°

[a] $N = 15.5$ for (d,p) and $29.5/(2J+1)$ for (d,^{3}He).

TABLE IV. Resume of ^{36}S(d,p)^{37}S angular distribution and cross section results. The choice of J^π is based on the l value unless otherwise noted.

No.	E_x (keV)	$\sigma_{max}^{c.m.}$ (μb/sr)[a]	θ_{lab}	l	$(2J_f+1)S$[b]	J^π
1	0	12 150	15	3	6.16	$\frac{7}{2}^-$[c]
2	644	19 900	10	1	2.62	$\frac{3}{2}^-$[c]
3	1395	830	10	2	0.22	$(\frac{3}{2},\frac{5}{2})^+$
4	1993	1670	10	1	0.15	$(\frac{3}{2})^-$[c]
5	2024	340	10	(3)	0.08	$(\frac{5}{2}^-,\frac{7}{2}^-)$
6	2517	460	20	(3)	0.14	$(\frac{5}{2}^-,\frac{7}{2}^-)$
7	2638	11 400	10	1	1.54	$\frac{1}{2}^-$[c]
8	3261	3650	10	1	0.60	$\frac{3}{2}^-$[c]
9	3356	730	10	>0		
10	3442	1120	10	>1		
11	3494	790	15	(1)	0.28	$(\frac{1}{2}^-,\frac{3}{2}^-)$
12	4008	840	10	>0		
13	4150	550	15[d]	>0		
14	4226	430	15[d]	>0		
15	4408	970	10	(4)	0.31	$(\frac{7}{2}^+,\frac{9}{2}^+)$
16	4813	1370	10	1,2		$(\frac{1}{2}\text{-}\frac{5}{2})$
17	4854	1890	10	1,2		$(\frac{1}{2}\text{-}\frac{5}{2})$
18	4883	1750	10	(1)	0.37	$(\frac{1}{2}^-,\frac{3}{2}^-)$
19	4903	580	10	>0		
20	5053	330	15[d]	>0		
21	5086	600	15[d]	>0		
22	5499	8120	10	3	1.2	$(\frac{5}{2},\frac{7}{2})^-$
23	5662	8060	10	>0		
24	5713	3450	10	>0		
25	6150	2270	10	>0		
26	6408	1950	15[d]	>0		

[a] The experimental uncertainty is estimated to be ~20%.
[b] The uncertainty in S is composed of 20% from experiment and a theoretical contribution representing the usual uncertainties in DWBA analysis of (d,p) data. A reasonable estimate is ~30% overall for bound states and perhaps ~50% for unbound states.
[c] The choice of J is from the proton analyzing power results of Ref. 5.
[d] Obscured at 10°.

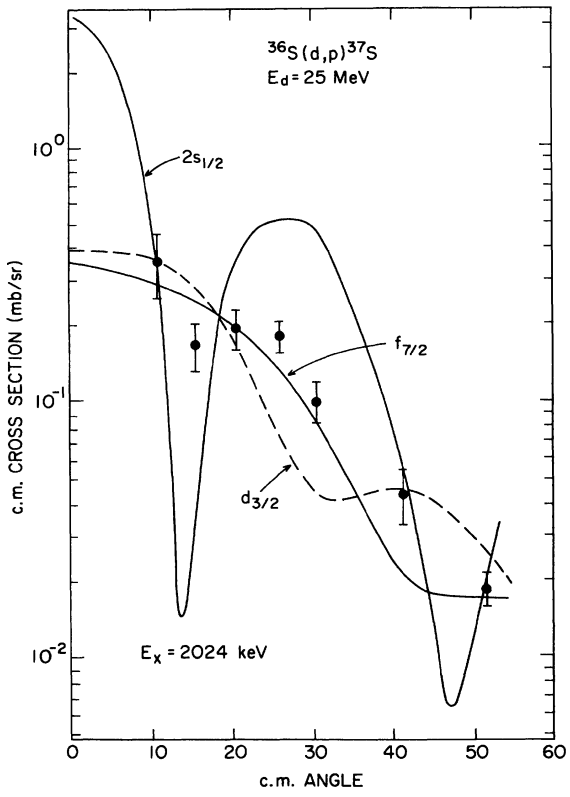

FIG. 4. Angular distribution for the ^{36}S(d,p)^{37}S 2024-keV level. The three theoretical curves are arbitrarily normalized. The cross section scale has an estimated uncertainty of 20%.

F. The ^{34,36}S(d,^{3}He)^{33,35}P results

A $\theta_{lab}=20°$ composite spectrum from five momentum slices is shown in Fig. 5. A further momentum slice at lower momentum (up to 7.3- and 9.6-MeV excitation in ^{35}P and ^{33}P, respectively) showed no evidence for any additional ^{33,35}P peaks. The energy resolution for this data on ^{35}P is ~32-keV FWHM. The background is largely due to non-^{3}He events and the discontinuities in the background level at the juncture between momentum slices is due to varying efficiency for rejection of these unwanted events which was made using the ΔE-E contour plot. The data shown were recorded just after a series of ^{36}S(d,p)^{37}S measurements and the (d,p) data provided a focal plane calibration. The results for the first three ^{33}P ^{3}He groups were also used for calibration. The uncertainty in the ^{35}P excitation energies is due almost entirely to uncertainties in the spectrometer field setting for that given slice. The ^{35}P ground-state Q value was obtained with relatively better accuracy because it appeared in the same momentum slice as the ^{33}P groups corresponding to the 1.43- and 1.85-MeV levels. A later series of measurements provided angular distribution points at six angles, but a focal plane calibration was not available for this second set of data nor were (d,^{3}He) results from an enriched ^{34}S target. The angular distribution data is illustrated in Figs. 6—8 and summarized in Table V.

The assignment of ^{3}He groups to ^{33}P and ^{35}P was done on the basis of the kinematical shift with angle. For instance, for the 5.06-MeV ^{33}P level, the difference between the ^{3}He energy for $\theta_{lab}=8°$ and 45° is 1007 keV, while if the group belonged to ^{35}P it would be 947 keV. These shifts differ by 60 keV and thus a plot of apparent excita-

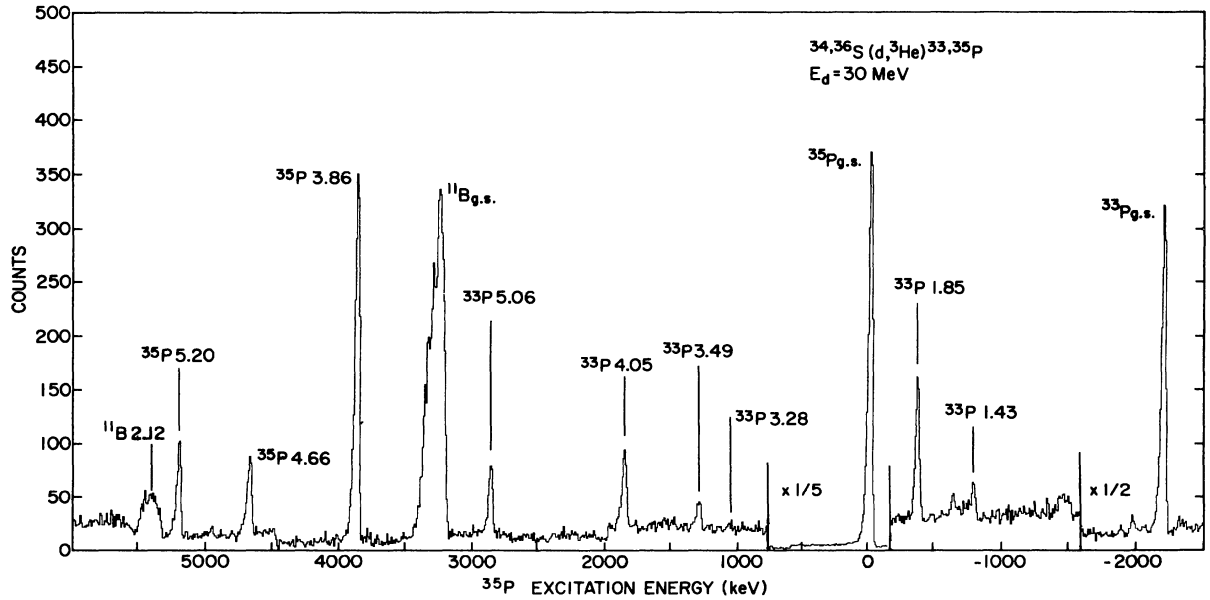

FIG. 5. ^{3}He spectrum from 30-MeV deuteron bombardment of the Ag_2S target. ^{33}P and ^{35}P peaks from ^{34,36}S + d are labeled by the excitation energies (in MeV) of the levels to which they correspond. Two ^{11}B peaks from ^{12}C(d,^{3}He) are also labeled.

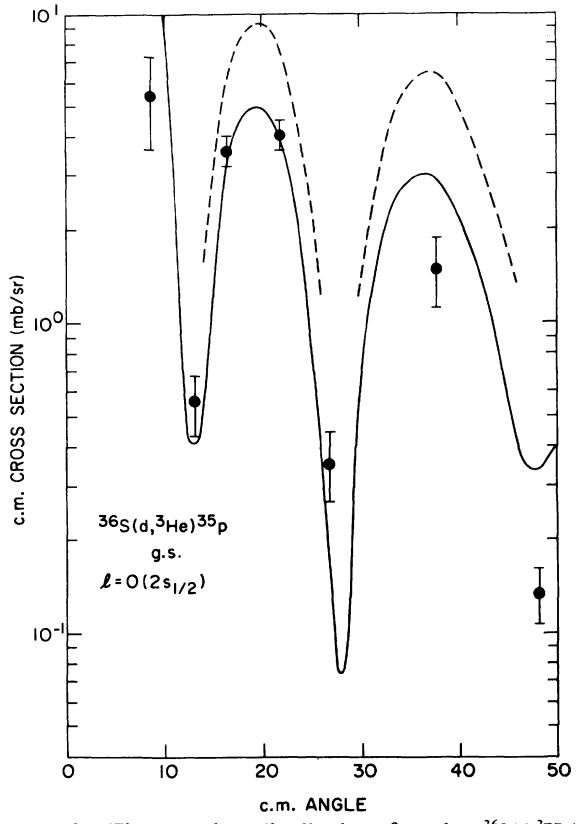

FIG. 6. The angular distribution for the ^{36}S(d,^{3}He)^{35}P ground-state reaction. The curves are DWUCK4 calculations for $l=0$ transfer. The solid curves correspond to the optical parameters of Table II. The dashed curve is for r_v(bound nucleus) $=1.3$ fm and $W(^{3}\text{He})=10.6$ MeV. The curves rise to 28 (solid) and 41 (dashed) mb/sr at 0°. Although the fit is not good, a definite $l=0$ assignment can be made.

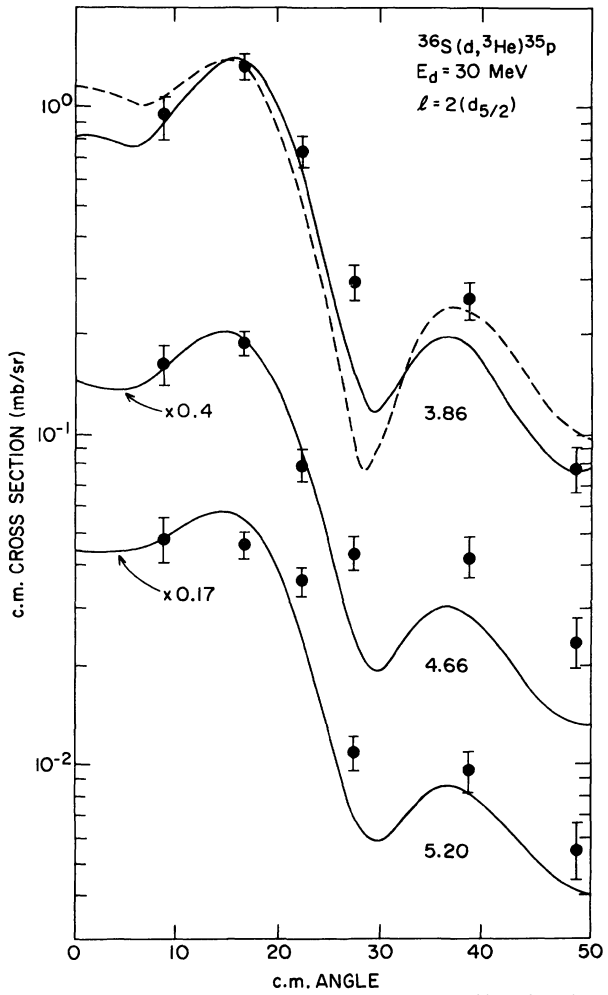

FIG. 7. Three $l=2$ angular distributions for ^{36}S(d,^{3}He)^{35}P. The distributions are labeled by the excitation energies (in MeV) of the ^{35}P states to which they correspond. The scale factors (e.g., $\times 0.4$) have been applied to the data. The solid curves are DWUCK4 calculations with the parameters of Table II, their normalization to the data yields the C^2S values of Table V. The dashed curve illustrates the effect of changes in the optical parameters (see Fig. 6).

tion energy versus angle for the assumption of a ^{33}P and ^{35}P final state provides an adequate distinction between the two: However, if a ^{33}P peak lies higher than a ^{35}P peak by ~ 30 keV at forward angles (so that the two peaks shift through each other as the angle is increased), the kinematical shift is not adequate to separate the two peaks if they differ significantly in intensity. It is therefore possible that one or more of the observed ^{33}P groups obscures a weaker ^{35}P group and vice versa. In any case, because of the relatively poor statistics and peak/background ratio [viz., the (d,p) results], only states with relatively large pickup strength were observed and others could easily have been missed.

As in other (d,^{3}He) angular distribution measurements, the quality of the DWUCK4 fits to the experimental angular distributions is not very good, especially at larger angles. However, it is adequate to fix the l transfer. This is so because of the clear distinction between various l values [in contrast to the (d,p) results]. The ^{35}P ground state is clearly $J^{\pi}=\frac{1}{2}^{+}$ although extraction of its spectroscopic strength has a large uncertainty due to the sensitivity of the magnitude of the $l=0$ second maximum with DWBA parameters. The remaining observed angular distributions—three each in ^{33}P and ^{35}P—are all assigned $l=2$ and have pickup strengths less sensitive to the DWBA parameters. The spectroscopic factors for the ^{33}P levels at 0, 1.43, and 1.85 MeV are estimated from the $\theta_{\text{lab}}=20°$ cross sections deduced from the data of Fig. 5. In our estimation, the uncertainty introduced in the C^2S values by the lack of angular distribution data is adequately covered by the uncertainty assigned to these C^2S values in Table V.

III. DISCUSSION

A. Comparison with previous results

1. ^{35}S(d,p)^{37}S

Previous results for ^{37}S include the excitation energies from the (d,p) results of Piskoř *et al.*[3] and Solin *et al.*[4] and the (t,^{3}He) results of Ajzenberg-Selove and Igo.[11]

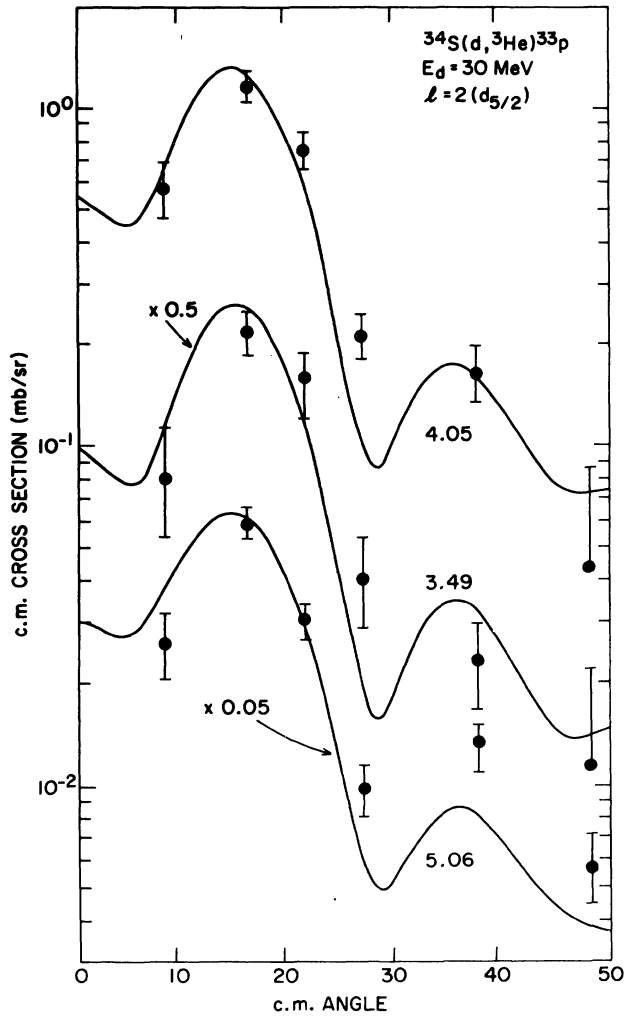

FIG. 8. Three $l=2$ angular distributions for ^{34}S(d,^{3}He)^{33}P. The distributions are labeled by the excitation energies of the ^{33}P states to which they correspond. The scale factors (e.g., $\times 0.5$) have been applied to the data. The solid curves are DWUCK4 calculations, their normalization to the data yields the C^2S values of Table V.

With all three of these there is excellent agreement with the observed states. Solin *et al.* reported a state at 1536 keV which was not observed by Piskoř *et al.* or in the present study. Since Solin *et al.* considered this state as uncertain and we studied the same reaction as they did, we consider it unlikely that such a state exists. The states at 2775 and 2978 keV, observed relatively strongly by Ajzenberg-Selove and Igo,[11] are candidates for high-spin or even-parity states, since such states would be expected to be formed very weakly in the (d,p) reaction. We discuss these states again in Sec. III B. Since we used the n,γ results as part of our energy calibration, it is not surprising that our energies are in good agreement with those of Ref. 1. The excitation energies of Piskoř *et al.*[3] are of comparable or better accuracy to ours and the agreement between the two sets of measurements is satisfactory. In the results of Piskoř *et al.*[3] there is a gap in the ^{37}S energy levels between 4.2 and 5.4 MeV (our states Nos. 14—21) which is unexplained. It is presumably related to the large number of impurities in the targets used by Piskoř *et al.*

Piskoř *et al.*[3] reported l and S values for ^{37}S states below 4 MeV. We have no disagreement with their l assignments, for all cases in which we find a definite assignment they do also. They do not quote a result for the 2024-keV level but give definite $l=1$, 3, and 1 assignments to the 3356-, 3442-, and 3494-keV levels for which we give incomplete results. The spectroscopic factors of Piskoř *et al.* and of the present results are in agreement well within the experimental uncertainties.

The Munich results[5] on ^{36}S(d,p)^{37}S have so far only appeared in an annual report. A gas target was used and the energy resolution was rather poor. However, proton analyzing power measurements were made thus allowing a choice between the two possible J values, $J=l\pm\frac{1}{2}$, in the ^{36}S(d,p)^{37}S stripping process. The J values chosen by this measurement are indicated in Table IV. In the case of the doublet at 1993—2024 keV, Kader *et al.*[5] (with their energy resolution) assigned to the 2024-keV level the $\frac{3}{2}^-$ determination we give to the 1993-keV level. Our reasoning is that the 1993-keV level is formed some 4.9 times more strongly than the 2024-keV level, and thus the data they observed (unresolved doublet) are characteristic of it rather than the 2024-keV level. For the 1395-keV level a clear preference for $l=2$ transfer over the $l=1$ ascribed by Kader *et al.*[5] is found by both Piskoř *et al.* and ourselves. Our other l transfer assignments are consistent with those of Kader *et al.*

2. ^{36}S(d,^{3}He)^{35}P

Previous results overlapping with the present ones exist only for the mass excess of ^{35}P. We find $-24854(5)$ keV as compared to $-24936(75)$ keV from a measurement[7] of the β^- end point in ^{35}P decay. The agreement is acceptable. The same β^- measurement established the ground state of ^{35}P as $J^\pi=\frac{1}{2}^+$ or $\frac{3}{2}^+$ in agreement with the present determination of $J^\pi=\frac{1}{2}^+$.

3. ^{34}S(d,^{3}He)^{33}P

The ^{34}S(d,^{3}He)^{33}P reaction was previously studied by Bearse, Youngblood, and Yntema[17] who measured angular distributions for the ^{33}P ground state and 1.85-MeV level at $E_d=23.4$ MeV. They reported spectroscopic parameters C^2S of 1.8 and 3.4 for these $l=0$ and 2 transfers. Using the identical optical parameters and procedure as for our 30-MeV data, we obtain C^2S values from their cross sections of 0.09 and 0.046; while—more appropriately—with the optical parameters listed by Bearse *et al.*, DWUCK4 yields $C^2S=0.13$ and 0.10, respectively. Clearly, the DWBA analysis of Bearse *et al.* is in error regardless of any comparison to the present experimental work. Now, invoking such a comparison, the peak cross sections reported by Bearse *et al.* of 0.18 and 0.07 μb/sr, respectively (see Fig. 5 of Ref. 17), for the ground state and the 1.85-MeV level must also be in error since

TABLE V. Resume of excitation energy, angular distribution, and cross section results for ^{34,36}S(d,^{3}He)^{33,35}P. For the ^{35}P levels and the 4.05- and 5.06-MeV ^{33}P levels the J^π values were deduced from the listed l values. For the other ^{33}P levels they are from Ref. 6.

E_x (keV)[a]	$\sigma_{max}^{c.m.}$ (mb/sr)[b]	θ_{lab}	l[c]	C^2S[d]	J^π
		^{35}P			
0[e]	4.00	20	0	2.3±1.2	$\frac{1}{2}^+$
3864(10)	1.35	15	2	1.45,1.10	$\frac{3}{2}^+,\frac{5}{2}^+$
4664(10)	0.47	15	2	0.53,0.41	$\frac{3}{2}^+,\frac{5}{2}^+$
5202(10)	0.28	15	2	0.40,0.30	$\frac{3}{2}^+,\frac{5}{2}^+$
		^{33}P			
0	5.7	20[f]	(0)	2.2	$\frac{1}{2}^+$
1431.6(2)	0.26	20[f]	(2)	0.37	$\frac{3}{2}^+$
1847.60(14)	1.20	20[f]	(2)	1.27	$\frac{5}{2}^+$
2538.6(7)	<0.08	15	(2)	<0.10	$\frac{3}{2}^+$
3275.4(9)	0.10(5)	15	(2)	0.06	$\frac{3}{2}^+,\frac{5}{2}^+$
3489.8(6)	0.43	15	2	0.19	$\frac{5}{2}^+$
3627.6(6)	<0.06	15	(4)		$\frac{7}{2}^+$
4047.8(8)	1.14	15	2	0.53,0.46	$\frac{3}{2}^+,\frac{5}{2}^+$
5060(10)	1.17	15	2	0.39,0.34	$\frac{3}{2}^+,\frac{5}{2}^+$

[a]Present values for the ^{35}P levels and 5.06-MeV level of ^{33}P. For the other ^{33}P levels the energies are from Ref. 6.

[b]The uncertainty is estimated as 20%.

[c]Values in parentheses result from the known values of J^π (Ref. 5).

[d]Unless otherwise noted the uncertainty is estimated as 50%. When two values are listed they are for the two J^π possibilities.

[e]The ^{36}S(d,^{3}He) Q value was measured to be −7606(4) keV corresponding to a ^{35}P mass excess of −24854(5) keV.

[f]Data taken at this angle only.

they result in spectroscopic factors some 10—24 times too small (compare Table V). We emphasize that these two errors, both of a factor >10, work in opposite directions. Thus, they are obscured by the fact that the resultant C^2S values are coincidentally reasonable.

The ^{33}P 5049-keV level has been given a definite spin assignment of $J=\frac{3}{2}$ from particle-γ correlation measurements in the ^{31}P(t,p)^{33}P reaction.[18] The correlation was performed on the γ-ray transition to the g.s., but γ transitions to the first two excited states were also reported and so it is possible that the 5049-keV level is actually a $J=\frac{3}{2},\frac{5}{2}$ doublet with the $\frac{3}{2}$ member contributing most of the γ transition to the g.s. in this measurement. Some slight evidence for this is provided by energy measurements[18] on the 5.05(doublet)→0 and 5.05(doublet)→1.85 transitions. Using[6] 1847.60(15) keV for the second-excited state of ^{33}P yields 5053.5(17) keV from the 5.05→1.85→0 γ-ray cascade, while the γ transition to the g.s. yields 5048.7(30) keV. The discrepancy is 4.8±3.4 keV. The question remains open, but the fact that essentially no $d_{3/2}$ strength is predicted in this energy range leads us to conclude that the level responsible for this strength might very well have $J^\pi=\frac{5}{2}^+$.

B. Comparison to expectations

1. ^{36}S(d,p)^{37}S

For ^{37}S there exists no theoretical calculation as to the level structure or (d,p) spectroscopic strengths. Here we compare our experimental results to local systematics in two ways. First, we apply the conventional weak-coupling approximation developed by Bansal and French[19] and Bernstein[20] for use near the ^{40}Ca closed shell. This is particularly simple to do for both ^{37}S and ^{35}P since, in view of the large neutron excess, we can neglect proton excitations in these nuclei. Thus, the low-lying levels of ^{37}S are, in this extreme model, comprised of ^{36}S⊗^{41}Ca, ^{35}S⊗^{42}Ca, and ^{34}S⊗^{43}Ca, where the symbol ⊗ represents extreme weak coupling of the energy levels of the two bodies. The predictions for the level positions (relative to the $\frac{7}{2}^-$ ground state from ^{36}S⊗^{41}Ca) are shown in the two level schemes on the left-hand side of Fig. 9. In this weak-coupling model, with no residual interaction, only the center of gravity of multiplets is predicted as is shown. In addition to the levels indicated in the figure this model would predict the other three

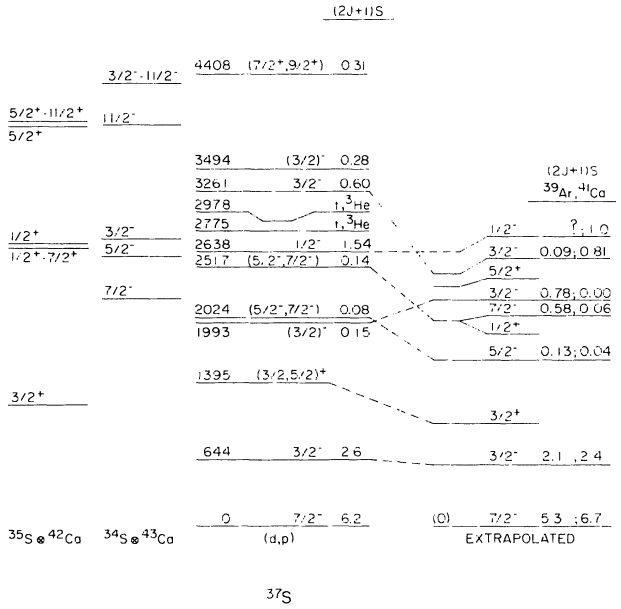

FIG. 9. Comparison of ^{37}S levels from ^{36}S(d,p)^{37}S to local systematics. Weak coupling results (Refs. 19 and 20) calculated with $a=-0.25$, $b=2.5$ MeV, are shown on the left-hand side of the experimental spectrum. The results on the right-hand side are from a linear extrapolation in the number of proton pairs for the low-lying levels of the $N=20$ isotones ^{41}Ca, ^{39}Ar, and ^{37}S. The spectroscopic strengths of the present experiment are shown for the $l=1$ and 3 distributions for $E_x<3.5$ MeV. The strengths are also listed for the analogous ^{39}Ar (Ref. 22) and ^{41}Ca (Ref. 23) levels.

single-particle levels of $\nu(1f_{7/2},2p_{3/2},2p_{1/2},1f_{5/2})$ as inferred from the experimental ^{41}Ca spectrum. These are hard to identify since the single-particle strength is fragmented and the relative single-particle energies are expected to vary with A. Thus, we also show the ^{37}S spectrum resulting from a linear extrapolation in the number of proton pairs using the ^{41}Ca and ^{39}Ar spectra from Ref. 6. These are shown on the right-hand side of Fig. 9. Except for the $\frac{3}{2}^-$ levels, only the lowest excited state of a given J^π is shown.

Both methods of comparing to local systematics do a good job of accounting for the observed states. The comparison offers strong evidence that several or more bound even-parity states were overlooked in the (d,p) measurements. The weak-coupling method predicts $\frac{1}{2}^+$, $\frac{1}{2}^+$, $\frac{3}{2}^+$, $\frac{5}{2}^+$, and $\frac{7}{2}^+$ states to be centered at $\sim$2.7 MeV and none of these states were observed. The extrapolation procedure is not possible for one $\frac{1}{2}^+$ state and the $\frac{7}{2}^+$ state, since these have not been located in ^{39}Ar (where the weak coupling model would predict them, cf. Ref. 21); it does predict $\frac{1}{2}^+$, $\frac{3}{2}^+$, and $\frac{5}{2}^+$ levels in this approximate energy region. The extrapolation procedure also failed for the lowest $\frac{1}{2}^-$ state since this state has also not been located in ^{39}Ar. In fact, with this state located in ^{37}S via the analyzing power results of Ref. 5, we can interpolate and predict a $\frac{1}{2}^-$ state with appreciable $2p_{1/2}$ strength at $\sim$3.2 MeV in ^{39}Ar. It may be that a $\frac{1}{2}^-$ state near this energy has been misidentified as $\frac{3}{2}^-$.

TABLE VI. Comparison of experimental and theoretical (Wildenthal) excitation energies and proton pickup strengths for the indicated ^{33}P and ^{35}P levels. Values of J^π in parentheses are assumed in order to agree with the theoretical predictions.

	E_x (keV)		C^2S	
J^π	(th)	(exp)	(th)	(exp)
		^{33}P		
$\frac{1}{2}^+$	0	0	1.27	$\sim$2.2
$\frac{3}{2}^+$	1531	1432	0.53	0.37
$\frac{5}{2}^+$	1997	1848	1.09	1.27
$\frac{3}{2}^+$	2646	2539	0.00	$<$0.10
$(\frac{3}{2}^+)$	3606	3275	0.02	$\sim$0.06
$\frac{5}{2}^+$	3787	3490	0.70	0.19
$\frac{7}{2}^+$		3628		a
$(\frac{5}{2}^+)$	3888	4048	1.31	0.46
$(\frac{5}{2}^+)$	5153	5060	1.34	0.34
		^{35}P		
$\frac{1}{2}^+$	0	0	1.76	$\sim$2.3
$\frac{3}{2}^+$	2652	a	0.12	a
$\frac{5}{2}^+$	4213	3864	5.51	1.10
$(\frac{5}{2}^+)$	b	4664	b	0.41
$(\frac{5}{2}^+)$	b	5202	b	0.30
$\frac{7}{2}^+$	7073	a		a
$\frac{5}{2}^+$	7053	a	0.05	a

[a]Not observed.
[b]These are presumably intruder states, i.e., not from $(2s1d)^{-5}$.

The inability to find even-parity states can be explained by their expected small spectroscopic strengths as inferred from those in ^{39}Ar and ^{41}Ca. It is possible that one or both of the states observed in (t,^{3}He), but not in (d,p), can be associated with two of these even-parity states.

The (d,p) strengths shown in Fig. 9 for ^{39}Ar and ^{41}Ca are from Refs. 22 and 23, respectively. The $l=1$ and 3 spectroscopic strengths shown for ^{41}Ca comprise 90% and 100% of the observed $2p_{3/2}$ and $1f_{7/2}$ strength below 4-MeV excitation. The summed strengths for $(2J+1)S$ in ^{41}Ca are 6.76, 0.04, and 3.21, and 1.0 for $f_{7/2}$, $f_{5/2}$, $2p_{3/2}$, and $2p_{1/2}$, respectively; for ^{37}S these strengths (with the assumed J^π values of Fig. 9) are 6.34, 0.14, 3.63, and 1.5, respectively. The similarity is startling.

2. ^{36}S(d,^{3}He)^{35}P

In Table VI and Fig. 10 comparison is shown of the (d,^{3}He) results to the $(2s,1d)^{-5}$ calculation of Wildenthal.[8] In Fig. 10 1p-6h and 2p-7h weak-coupling predictions are also included. Aside from the $l=0$ transition to the $J^\pi=\frac{1}{2}^+$ ground state, most of the spectroscopic strength is predicted to reside in the $l=2$ transition to the lowest-lying $\frac{5}{2}^+$ state. Only three excited states were observed

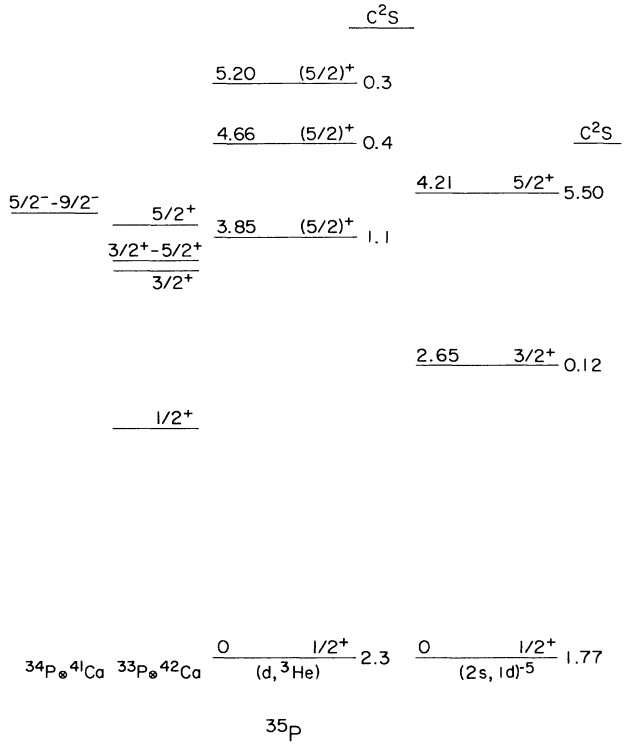

FIG. 10. Comparison of the ^{35}P levels from ^{36}S(d,^{3}He)^{35}P to weak coupling results and the $(s,d)^{-5}$ calculations of Wildenthal (Ref. 8). The (d,^{3}He) pickup strength C^2S is shown for the $(s,d)^{-5}$ calculation as well as for experiment.

and it is assumed that these are all $\frac{5}{2}^+$ states which share part of the predicted $l=2$ strength. The $(2s,1d)^{-5}$ state is then fragmented via mixing with 2p-7h states. The two lowest states predicted are included in Fig. 10. Since the observed $l=2$ strength is considerably less than that predicted, it would appear that considerable $d_{5/2}$ pickup strength is to be found at higher excitation energy.

The present experiment was quite selective with little sensitivity for states with small C^2S values. From inspection of Fig. 10 it would appear that numerous other states in ^{35}P below 5-MeV excitation remain to be found.

3. $^{34}S(d,^3He)^{33}P$

In Table VI are listed the spectroscopic strengths resulting from analysis of the (d,^{3}He) cross sections using DWUCK4 with the parameters of Table II. Comparison to Wildenthal's $(s,d)^{-7}$ calculation indicates quite good agreement up to the $(\frac{3}{2}^+)$ 3275-keV level. Above that, the experimental $d_{5/2}$ pickup strength is 30% of that predicted. As in the case of ^{35}P, it is probable that the strength is shared with intruder states and its centroid is pushed to higher energy.

C. Understanding thermal neutron capture

In the off-resonance situation, direct capture effects play a strong role in thermal neutron capture and the observed primary γ-ray partial cross sections[1] can be compared with the model predictions. According to Lane and Lynn,[24] the predicted cross sections (in barns) are given by[25]

$$\sigma_\gamma \approx \sigma(\mathrm{hs}) C \ , \tag{3}$$

where the hard sphere (hs) cross section is

$$\sigma(\mathrm{hs}) \approx \frac{0.062}{R\sqrt{E_n}} \left[\frac{Z}{A}\right]^2 \frac{(2J+1)S}{6} y^2 \left[\frac{y+3}{y+1}\right]^2 , \tag{4}$$

and the factor C is

$$C \approx \left[1+\frac{R-b_s}{R} y \left[\frac{y+2}{y+3}\right]\right]^2 . \tag{5}$$

In the above expressions, R is the nuclear potential radius in fm, $y=kR$, $k=0.219\sqrt{E_\gamma(\mathrm{MeV})}$ fm^{-1}, E_γ is the primary γ-ray energy, and b_s is the scattering length in fm. It is customary to define the potential radius as $R=1.35A^{1/3}$ fm which reduces to 4.5 fm for ^{37}S. All quantities required to evaluate Eqs. (3)—(5) are now known except for the scattering length b_s. In Table VII, we show a comparison between the measured and calculated values. The agreement is excellent if b_s is assumed to be 3.0 fm, and still reasonable (i.e., within 20%) if b_s is 2.5 or 3.5 fm. Only a future experiment, such as the one carried out on the other three stable S isotopes (^{32}S, ^{33}S, and ^{34}S) by Koester, Knopf, and Waschkowski[26] can yield

TABLE VII. Comparison between measured and calculated thermal neutron capture cross sections in ^{37}S.

E_x (keV)	J^π	$(2J+1)S$[a]	Primary E_γ (keV)	Measured[b] σ_γ (mb)	Calculated[c] σ_γ (mb) $b_s=2.5$ fm	σ_γ (mb) $b_s=3.0$ fm	σ_γ (mb) $b_s=3.5$ fm
646	$\frac{3}{2}^-$	2.71	3657	161 ±18	207	168	132
1992	$\frac{3}{2}^-$	0.22	2312	9.4± 1.2	10.0	8.3	6.9
2638	$\frac{1}{2}^-$	1.60	1666	52 ± 7	51	43	37
3262	$\frac{3}{2}^-$	0.58	1042	8.1± 1.0	11.3	9.9	8.6
3493	$(\frac{1}{2}^-,\frac{3}{2}^-)$	0.31	811	2.4± 0.3	4.8	4.2	3.7
			$\sum\sigma_\gamma$ (mb)=232.9		274.1	233.4	188.2

[a]Average of current values and those from Ref. 3.

[b]From Ref. 1.

[c]From Eqs. (3)—(5).

information on the correct scattering length.

Another prediction of the direct capture theory is that the capture cross section is nearly proportional to the first power of the γ-ray energy rather than to its cube. The latter is the usual assumption for the energy behavior of dipole transitions. In the current case, the correlation coefficient between the capture cross sections (to specific states) divided by the γ-ray energy and the spectroscopic strength is 0.99, in agreement with these expectations.

The excellent overall agreement between experiment and direct capture theory noted here for ^{37}S extends also to the cases of ^{33}S (Ref. 25) and ^{35}S (Ref. 27).

ACKNOWLEDGMENTS

We would like to thank B. H. Wildenthal for providing us with the results of his (*s,d*) calculations for ^{33}P and ^{35}P and for discussions concerning them. We thank W. Ratynski for facilitating the acquisition of enriched ^{36}S. The targets were made by Micha Petek and we thank her. This research was supported by the U.S. Department of Energy, Division of Basic Energy Sciences under Contract No. DE-AC02-76CH00016 with the Associated Universities, Inc. (BNL), and No. DE-AC05-840R21400 with the Martin Marietta Energy Systems (ORNL).

[1]S. Raman, W. Ratynski, E. T. Jurney, M. E. Bunker, and J. W. Starner, Phys. Rev. C **30**, 26 (1984).

[2]S. Raman, C. Thorn, J. W. Olness, and E. K. Warburton, *Proceedings of the International Conference on Nuclear Physics, Florence, 1983* (Tipografia Compositori, Bologna, Italy, 1983), Vol. I, p. 246.

[3]Š. Piskoř, P. Franc, J. Křemének, and W. Schäferlingová, Nucl. Phys. **A414**, 219 (1984).

[4]L. M. Solin, YuA. Nemilov, V. N. Kuz'min, and K. I. Zherebtsova, Yad. Fiz. **29**, 289 (1979) [Sov. J. Nucl. Phys. **29**, 143 (1979)].

[5]H. Kader, H. Clement, G. Graw, H. J. Maier, F. Merz. N. Seichert, and P. Schiemenz, Jahresbericht, Technischen Universität München Annual Report, 1982, p. 33.

[6]P. M. Endt and C. Van der Leun, Nucl. Phys. **310**, 1 (1978).

[7]D. R. Goosman and D. E. Alburger, Phys. Rev. C **6**, 820 (1972).

[8]B. H. Wildenthal, private communication.

[9]G. A. P. Engelbertink and J. W. Olness, Phys. Rev. C **3**, 180 (1971).

[10]E. Beardsworth, J. Fischer, S. Iwata, M. J. LeVine, V. Radeka, and C. E. Thorn, Nucl. Instrum. Methods **127**, 29 (1975).

[11]F. Ajzenberg-Selove and G. Igo, Nucl. Phys. **A142**, 641 (1970).

[12]C. E. Thorn, W. F. Piel, M. J. LeVine, P. D. Bond, and A. Gallmann, Phys. Rev. C **25**, 331 (1982).

[13]P. D. Kunz, University of Colorado report (unpublished).

[14]W. W. Daehnick, J. D. Childs, and Z. Vrcelj, Phys. Rev. C **21**, 2253 (1980).

[15]F. Fabrici, S. Micheletti, M. Pignanelli, F. G. Resmini, R. De Leo, G. D'Erasmo, A. Pantaleo, J. L. Escudié, and A. Tarrats, Phys. Rev. C **21**, 830 (1980).

[16]P. Doll, H. Mackh, G. Mairle, and G. J. Wagner, Nucl. Phys. **A230**, 329 (1974).

[17]R. C. Bearse, D. H. Youngblood, and J. L. Yntema, Phys. Rev. **167**, 1043 (1968).

[18]A. R. Poletti, T. T. Bardin, J. C. Pronko, and R. E. McDonald, Phys. Rev. C **7**, 1433 (1973); **7**, 1479 (1973).

[19]R. K. Bansal and J. B. French, Phys. Lett. **11**, 145 (1965).

[20]A. M. Bernstein, Ann. Phys. (N.Y.) **69**, 19 (1972).

[21]E. K. Warburton, J. W. Olness, J. J. Kolata, and A. R. Poletti, Phys. Rev. C **13**, 1762 (1976).

[22]S. Sen, C. L. Hollas, C. W. Bjork, and P. J. Riley, Phys. Rev. C **5**, 1278 (1972).

[23]G. Brown, A. Denning, and J. G. B. Haigh, Nucl. Phys. **A225**, 267 (1974).

[24]A. M. Lane and J. E. Lynn, Nucl. Phys. **17**, 563 (1960); **17**, 586 (1960).

[25]S. Raman, in *Neutron Capture Gamma Ray Spectroscopy and Related Topics 1981*, edited by T. von Egidy, F. Gönnenwein, and B. Maier (Institute of Physics, Bristol, 1982), p. 357.

[26]L. Koester, K. Knopf, and W. Waschkowski, Z. Phys. A **289**, 309 (1979).

[27]R. F. Carlton, S. Raman, and E. T. Jurney, in Ref. 24, p. 375.